Turkish Journal of Earth Sciences
http://journals.tubitak.gov.tr/earth/
Research Article

Turkish J Earth Sci
(2023) 32: 96-112
© TÜBİTAK
doi:10.55730/1300-0985.1829

Evidence for surface rupture of the 1939 Erzincan earthquake based on field data and paleoseismology on the Ezinepazarı Fault (North Anatolian Fault Zone, Central Anatolia)

Fikret KOÇBULUT*
Department of Geology, Sivas Cumhuriyet University, Sivas, Turkey

Received: 15.10.2022 • **Accepted/Published Online:** 21.12.2022 • **Final Version:** 19.01.2023

Abstract: The Ezinepazarı Fault (EPF) is an active segment that restricts the Niksar Basin in the central part of the North Anatolian Fault Zone and has been the source of the devastating Mw 8.0 earthquake in the last 100 years. Traces of the surface rupture of the EPF, which occurred in AD 1939, can still be observed in the field today as a right-lateral strike-slip character. While paleoseismological studies were mostly focused on the western part of the North Anatolian Fault Zone (NAFZ) in previous studies, the studies on the central and eastern parts of the NAFZ are rarely addressed. In this context, trench-based paleoseismology studies were carried out on the surface rupture traces in order to determine both historical/prehistoric earthquakes caused by the fault and the Quaternary period characteristics of the EPF. According to the data obtained, at least two historical earthquake activities have been detected besides the last 1939 earthquake on the EPF. Accordingly, the first and second events occurred in E1: 5871 ± 2300 BP and E2: 1651 ± 128 BP, respectively. When the determined data are compared with the historical earthquake catalogs, it is concluded that Event 2 (E2) can be correlated with the AD 343 Niksar earthquake; thus, the EPF has an irregular earthquake recurrence interval.

Key words: Ezinepazarı Fault, North Anatolian Fault Zone, surface rupture, paleoseismology

1. Introduction

As a result of the 26 December 1939 Erzincan earthquake (Mw: 7.9–8.0), which was the largest earthquake in the last century, a surface rupture of 360 km developed along a zone stretching from Erzincan to Amasya and caused the death of nearly 33,000 people (Pamir and Ketin 1941, Parejas et al., 1942, Ketin 1969). On the surface rupture, besides the right lateral offsets of 3.7 to 7.5 m, which reflect the character of the fault, the vertical offsets of 0.5–2 m were also detected (Ketin 1969, Koçyiğit 1989, Barka 1996, Gürsoy et al., 2013). Detailed mapping studies were not carried out on the surface rupture, except for the area between Suşehri and Erzincan (Koçyiğit and Tokay 1985; Koçyiğit, 1989), Reşadiye (Seymen 1975) and Koyulhisar (Toprak 1989) district centers. Barka (1996) made local observations on the amount of displacement on the surface rupture between the years 1939 and 1967 along the fault belt. In addition to that, significant paleoseismological studies were carried out on the 1939 earthquake surface rupture (Hartleb et al. 2006, Fraser et al. 2012, Kozacı et al. 2011; Zabçı et al. 2011, Kondo et al. 2012; Hubert-Ferrari et al. 2012; Tatar et al. 2012; Polat et al., 2012, Gürsoy et al. 2013, Emre et al., 2020). From these researchers, Gürsoy et al. (2013) made new observations on the 1939 Erzincan earthquake surface along the Kelkit valley. Recently, Emre et al. (2020) investigated the fault geometry, segmentation, and slip distribution associated with the 1939 earthquake on the North Anatolian Fault Zone. Moreover, they state that the rupture propagation through EPZ from the main strand of NAFZ can be driven by a number of factors such as rupture direction, fault geometry and the magnitude of stress transferred at the segment boundary. Furthermore, their analysis regarding the rupture geometry and slip distribution in the 1939 earthquake has implied that it is source fault characterization of similar multisegment strike-slip faults.

However, in the approximately 40 km section between Köklüce (SE Niksar) and Fındıcak villages, the traces of the surface rupture have not been studied yet in detail. In this study, some very distinctive morphotectonic structures are observed and mapped and paleoseismology studies were carried out between Köklüce village and Fındıcak further west, in order to determine the current traces of the surface rupture formed by the 1939 earthquake and to determine the historical earthquakes that developed on this segment.

2. Seismotectonic settings

The North Anatolian Fault Zone (NAFZ), which is mainly classified into three zones as such the Eastern, the Central,

* Correspondence: fbulut@cumhuriyet.edu.tr

and the Western, is a right-lateral strike-slip transform fault system that separates the Eurasian and Anatolian plates regionally (Emre et al., 2013; 2018) (Figure 1).

The overall NAFZ consists of 38 segments, the eastern part of NAFZ is divided into 8 segments, which are Kargapazarı, Elmalı, Yedisu, Erzincan, Refahiye, Reşadiye, and Ezinepazarı segments (Emre at al., 2018) (Figure 1). Since the historical period, many earthquakes have occurred in the last 100 years, affecting the working area of the Ezinepazarı Fault and its surroundings, causing loss of life and property. These earthquakes are observed as clusters in certain regions. Especially in terms of historical earthquakes, there are catalogs of the existence of a number of historical earthquakes in the immediate vicinity of the NAFZ-Ezinepazarı segment, from AD 236 earthquake to AD 1776 earthquake (e.g., Ambraseys 1970; Ambraseys and Finkel 1987, 1995; Ambraseys and Melville 1994; Eyidoğan et al., 1991; Guidoboni et al., 1994; Guidoboni and Comastri, 2005, Tan et al., 2008).

From these earthquakes, the AD 236 earthquake mentioned in the catalog of Guidoboni et al. (1994) comes from an inscription dated AD 235–236. This earthquake could be detected in Alayurt trench opened near the basin (Hartleb et al., 2003), and Aslançayırı trench in its west (Yoshioka et al., 2000). Thus, although its exact extent is not known, it was concluded that the AD 236 earthquake was a major earthquake that caused a surface rupture on the NAFZ (Erturaç and Tüysüz, 2012).

According to Guidoboni and Comastri (2005), the AD 343 Niksar earthquake caused very severe damage to the city, except for the church, the episcopal palace, and those inside. Another severe earthquake is AD 499 Suşehri earthquake that severely shook Suşehri and the surroundings of Niksar. Suşehri became a ruin after this earthquake that took place at midnight. While the earthquake was felt throughout the Black Sea Region, Niksar also suffered great damage (Guidoboni et al., 1994).

The AD 1035-1045-1050 earthquake series are an earthquake series in the western (1035), eastern (1045), and central (1050) parts of the NAFZ, of which the possible extension of the surface rupture was determined by the damage distribution and paleoseismological trench studies with the help of historical sources. The 1034 and/or 1035 earthquakes are recorded in historical records as an earthquake with devastating effects in Ankara and its north and possibly around Bolu (Guidoboni and Comastri, 2005). The surface rupture of the earthquake was found in the Gerede and Demirtepe trenches (Hartleb et al., 2006). The 1045 earthquake was experienced as a very severe earthquake in and around the present Erzincan Province.

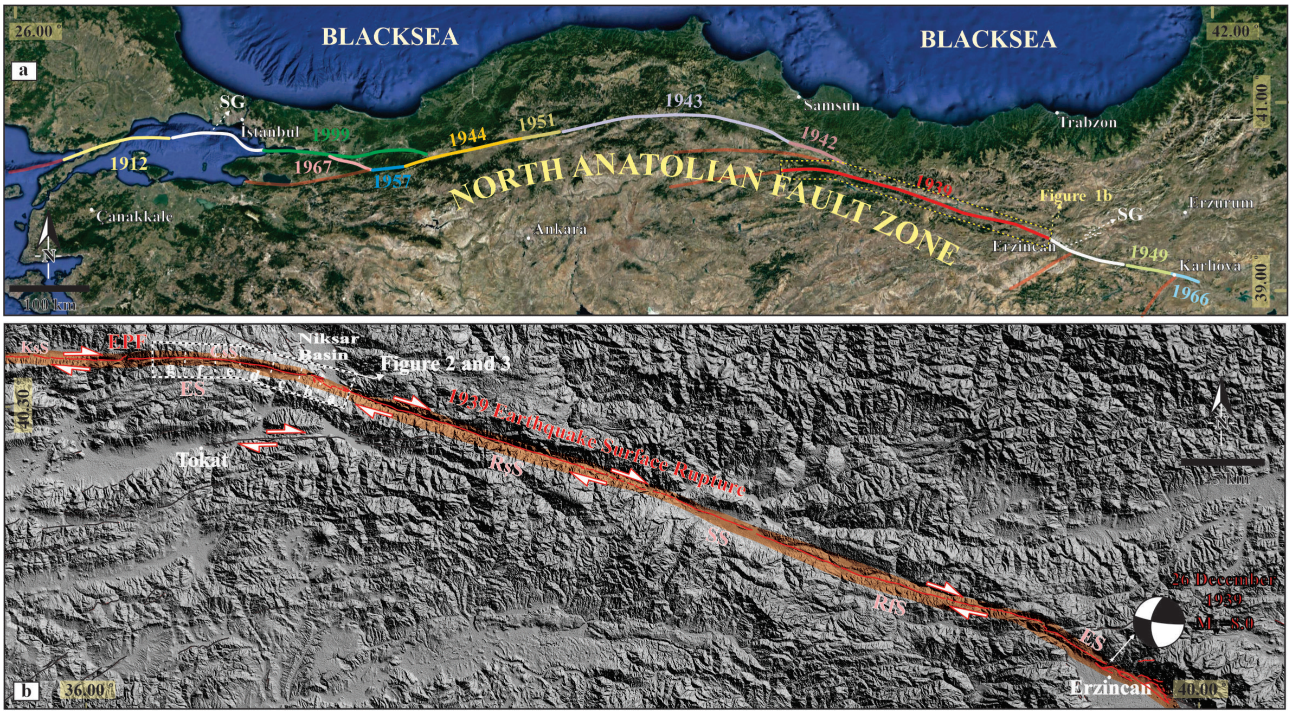

Figure 1. a) The surface rupturing earthquakes along the North Anatolian Fault (modified from Emre at al., 2020). b) The map of the surface rupture along the NAFZ on 1939 Erzincan earthquakes. The red lines under the black-red shaded and black lines shows active faults redrawn from Emre et al. (2013). The focal mechanism of Erzincan earthquake is taken from McKenzie (1972). EPF: Ezinepazari Fault, ES: Ezinepazari Segment, RsS: Reşadiye Segment, SS: Suşehri Segment, RfS: Refahiye Segment, ES: Erzincan Segment, CsS: Canbolat Subsegment, KsS: Karataş Subsegment, SG: Seismic Gap.

Many houses and churches in the surrounding areas were in ruins. Aftershocks continued to affect the region for about a year, possibly lasting until March 6, 1046. It is reported that deep rifts were formed and the city was almost completely destroyed (Guidoboni and Traina, 1995; Guidoboni and Comastri, 2005). In other catalogs, it is stated that this big earthquake took place on April 5, 1045 (Ambraseys and Jackson, 1998).

According to Guidoboni and Comastri (2005), the 11 October 1254 Erzincan earthquake; an area stretching from Erzincan to Niksar (Sebaste) was damaged by a very strong earthquake. Towards the west of Erzincan, the surface rupture and associated landslides have occurred along the Kelkit valley. Another interpretation based on all the historical data is that the surface faulting extending up to Erzincan should be around 150 km in total. According to this approach, the earthquake epicenter is around Suşehri (Ambraseys and Melville, 1995). Kondorskaya and Ulomov (1999) drew attention to the existence of the March 1419 Tosya earthquake; which is not included in major known catalogues. According to this source, which does not contain much data on destruction and surface faulting, the magnitude of the earthquake is 7.6. According to Ambraseys and Finkel (1995), an earthquake in Çorum on October 19, 1579 destroyed many houses and caused significant damage to public buildings.

During the AD 1668 earthquake (Large Anatolian Earthquake), the NAFZ between Niksar and Bolu was completely broken according to the impact area assessments. The highest intensity of this earthquake is XI (M: 8) (Ambraseys and Finkel, 1995). The extent of this earthquake's surface rupture was determined by trench studies (e.g., Yoshioka et al., 2000; Hartleb et al., 2003; Fraser et al., 2009; 2012; Kondo et al., 2012; Avsar et al., 2014). The last historical earthquake that occurred on NAFZ is the AD 1776 earthquake. Amasya (Vezirköprü) and Çorum provinces were affected and many buildings in the region were destroyed (Ambraseys and Finkel, 1995). In addition to these settlements, which are very close to the main branch of the NAFZ and located on young sediments, a damaged tomb was destroyed in Amasya (Yaşar, 1912, 1928).

2.1. Ezinepazarı Fault (EPF)

The Ezinepazarı Fault (EPF), first identified by Ketin (1969) after the field studies following the 1939 Erzincan earthquake as a right lateral strike-slip fault, restricts the southern edge of the Niksar basin and then changes its direction and continues westward in the E-W extension. According to Barka (1996)'s suggestion, the 1939 earthquake rupture was divided into 5 segments based on discontinuities such as stepovers, bends, and slip distributions. After that, Emre et al. (2013) and Emre et al. (2018) were grouped into the same five morphological segments considering McCalpin's (1996) behavioral segment definitions, which are Erzincan, Refahiye, Suşehri, Reşadiye, and Ezinepazarı segments. The Ezinepazarı segment consists of two morphological sections that lay on the westernmost of the 1939 earthquake. Emre et al. (2020) state that these sections, namely Karataş and Canbolat, are merged with a restraining stepover. The eastern, 56-km long Canbolat section is the main body of the segment. The western 20-km-long Karataş section forms the western end of both the segment and the 1939 earthquake rupture zone. The Canbolat section is slightly concave to the south while the Karataş section is almost straight with an E-W orientation.

The Ezinepazari Fault has two stepover zones that were determined along the 40 km surface rupture in the 1939 earthquake (Emre et al., 2013; 2018; 2020). These stepover zones are filled by Upper Pliocene terrestrial deposits which are composed of loosely cemented terrestrial sediments. The basement of the basin is formed by the Permo-Triassic Turhal group (Figure 2). It consists of mostly mafic magmatic rocks and recrystallized limestone blocks. The youngest Quaternary rocks overlie all units with an angular unconformity.

3. Methodology

In this study, approximately 40 km of the surface rupture in the south of Niksar-Erbaa, which was formed as a result of the 1939 Erzincan earthquake, was mapped and morphotectonic elements such as stream offsets, source sequences, slopes, collapse structures such as sag ponds, pressure ridges, and landslides were investigated. In this context, firstly, the geological mapping at 1/25,000 scale, geomorphological investigations, and then paleoseismological trench studies were carried out on the Ezinepazarı segment in accordance with McCalpin's (1996) methodology. Samples taken from earthquake-related event horizons were sent to the Geochron Laboratory (Mass-USA) and the results were evaluated in the Oxcal program.

4. Findings

4.1. Field observation on the Ezinepazarı Fault

In this study, the surface rupture between near Gölönü village and near the Şaryeri region was examined in three parts (Figures 2 and 3). The first surface rupture, observed along 6 km in the study area, extends approximately in the N65W direction in the form of a narrow zone at the southeast end of the Niksar Basin. It runs parallel to the Kelkit Stream in Eskideğirmen-Şaryeri locality, cuts the main road from the north of Köklüce village, and enters the Kelkit Riverbed from the northern slope of Maltepe in the northeast of Camidere village (Figure 3a). The Kelkit River changes its direction in this region. These riverbed changes are thought to be the result of historical earthquakes in the

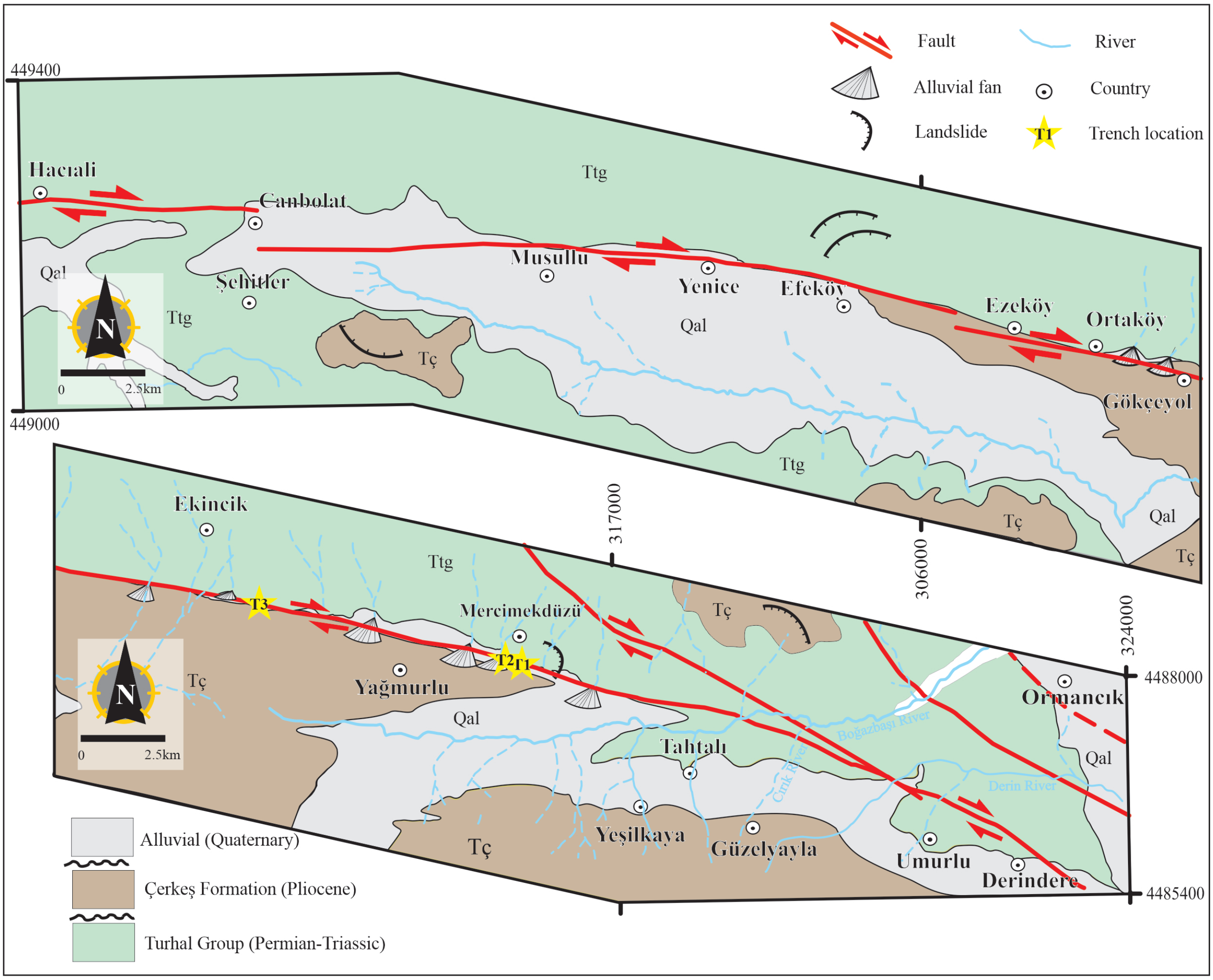

Figure 2. The general 1/25k scaled geological map between Haciali and Derindere villages along the EPF. Yellow stars represent trench locations.

region. As a matter of fact, it was stated by the people living in the region where the water of the river was cut off for a certain period of time in the 1939 earthquake.

The segment extends towards the river bed of the Kelkit River by cutting the main road around Maltepe, north of Camidere village, in the direction of N75W towards the west. From here, it jumps to the left and continues from the west of Korulu village. Continuing into the Niksar basin in one branch, it exhibits a geometry parallel to the extension of the 1942 surface rupture.

The second part, which is 25-km-long, the surface rupture jumps approximately 1 km to the left and extends in the N75W direction, west of Korulu village. It reaches the Yağmurlu village by passing 50 m northern slope of Devedüzü Tepe (hill), north of Umurlu and Yeşilkaya villages, between Silemiş Tepe and Korucu Tepe in the northeast of the Derindere village.

The surface rupture extending in the N75W direction to the west of the Korulu village continues to the west, passing through the Köklüce hydroelectrical power plant (HEPP) and Çermikbaşı region (Figure 3b). Travertines are observed in the Çermikbaşı region as a result of the outflow of hot water. Continuing to the west from the southern slope of Silemiş Tepe in the NE of the Derindere village, the surface rupture extends from the north of Derindere to the north of the Umurlu village. In the northwest of the Umurlu village, possible tension cracks with a strike of N40°W and their deep traces can be seen. Similarly, the rupture that continues in the N85°W direction along Cırıkdere, the west of Umurlu village, passes the 50 m north slope of Devedüzü Tepe, cuts the Tokat-Niksar highway along the stream north of Akyüzü ridge and Harmancık ridge, and reaches the Yağmurlu village (Figures 3b, 3c, and 4).

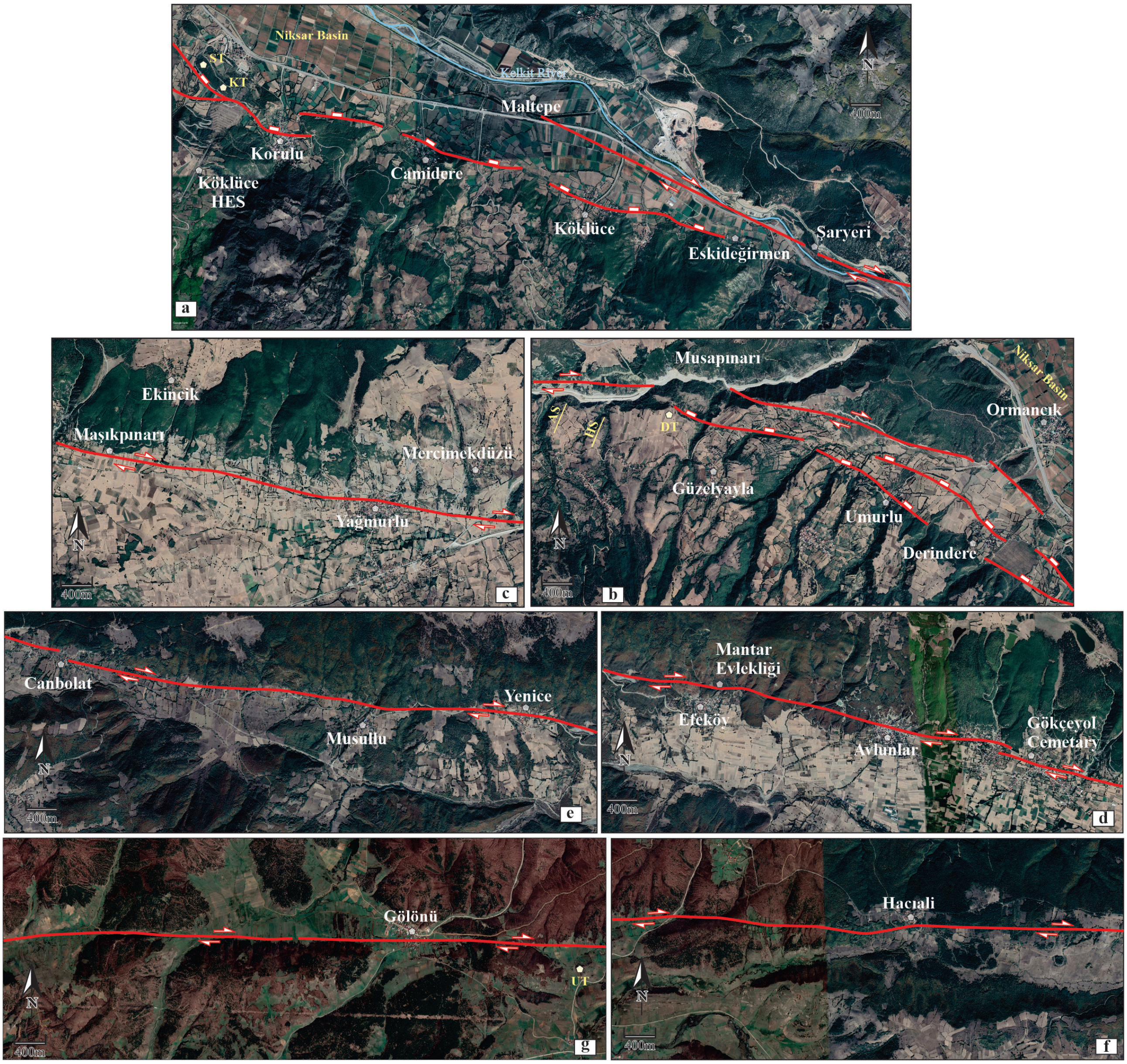

Figure 3. The detailed geometry and segment features of Ezinepazarı segment between near Gölönü and Şaryeri villages. The red lines show active faults redrawn from Emre et al. (2013). The Google earth images were used to illustrate relevant segments. KT: Korucu Tepe (hill), ST: Silemiş Tepe, DT: Devedüzü Tepe, HS: Harmancık Sırtı, AS: Akyüzü Sırtı, UT: Uyku Tepe.

To the west of the Yağmurlu village, the trace of the surface rupture continues in the N75°W direction. Displaced stream and elongated ridge morphologies are well observed. In the continuation of these structures, it was observed that the fault has a right lateral strike-slip character with strikes ranging from N74W to E-W in the Maşık Pınarı region, the south of Ambarcık Tepe, to the west. From here, the fault passes through Gökçeyol, Ortaköy, Ezeköy, and Efeköy to the west (Figure 3d). To the east of Gökçeyol village, the fault plane extending in the N74W direction and the slip striations on them show that the fault has a right lateral strike-slip character with a very small amount of normal component.

The first fault plane in this area is N74W/ 88NE, a right-lateral strike-slip fault and slip striations with rake angle of 15NW have developed on the plane. Besides, the second fault with an N65°W strike and 85SW dip is a right-lateral strike-slip fault with rake angle of 28 SW. In the river between the mosque and the cemetery in Gökçeyol village, a displacement of approximately 25 m has been

Figure 4. Distribution of Ezinepazarı fault, which caused the 1939 earthquake, between Umurlu and Yağmurlu villages. A) The 1939 fault trace extending in N75W direction in the NW of Umurlu village; B): C) The view from the elongated ridge morphology of the surface fracture in south of Canbolat village; looking South.

determined (Figures 5c and 5d). After the surface rupture of the 1939 earthquake displaces this river, it continues westward through the village cemetery towards Ortaköy.

The 20-cm right lateral displacement in the form of a crypt on the west wall of the Gökçeyol village cemetery has taken place in approximately 20 years. This gives a movement rate of 1 cm per year. The trace of the surface rupture in Ortaköy, Ezeköy, and Efeköy regions is in the N75W direction, through Ortaköy and Ezeköy, and the surface rupture with the strike of N50W in Efeköy, at the Mantar Evlekliği locality, can be seen even today (Figures 5 a and 5b). Although 83 years have passed, the cut in the fracture scar has not closed. Morphotectonic elements such as river and ridge displacements, source sequences, and subsidence structures such as sag ponds, pressure ridges, and landslides belonging to the 1939 surface rupture are well seen in that locality. The surface rupture extends in an N70W direction up to the Yenice village and N80°W up to the south of Musullu, Köseli, and Canpolat villages (Figure 3e).

The third part of the surface fracture has a length of 18 km. In this region, the fracture continues to the west by jumping to the right. A sag pond formed in the stepover zone. In previous studies, the offsets of 2–2.25 m in Canpolat village and 1.75 m in Fındıcak village were reported on this segment of the 1939 surface rupture (Barka 1996).

The fracture extending in the E-W direction from the pine forest to the west in the north of the Canpolat village is clearly visible in the meadow area on the side of the Erbaa road to the west of the village. Small sag ponds are seen on the fault and these areas maintain their greenery. It reaches the Gölönü village from the northern slope of Uyku Tepe, south of Hacıali village, and north of Sokutaş village. It can be traced from Gölönü to the west and from Çamlık Tepe to the north of Fındıcak village (Figures 3f and 3g).

4.2. Paleoseismological studies

While relatively many paleoseismological studies have been conducted in the western part of the NAFZ, the eastern part is poorer in this respect (Barka, 2000; Hartleb et al., 2002; Hitchcock et al., 2003; Klinger et al., 2003; Hartleb et al., 2006a; Pavlides et al., 2006; Palyvos et al., 2007; Pantosti et al., 2008). Within the scope of this study, trenches for paleoseismology was opened at three different locations on the Ezinepazarı Fault of the 1939 earthquake rupture (between Köklüce and Fındıcak) and sampling was made for ^{14}C dating in three of these trenches. The age data were obtained by the ^{14}C analysis of the earthquake-

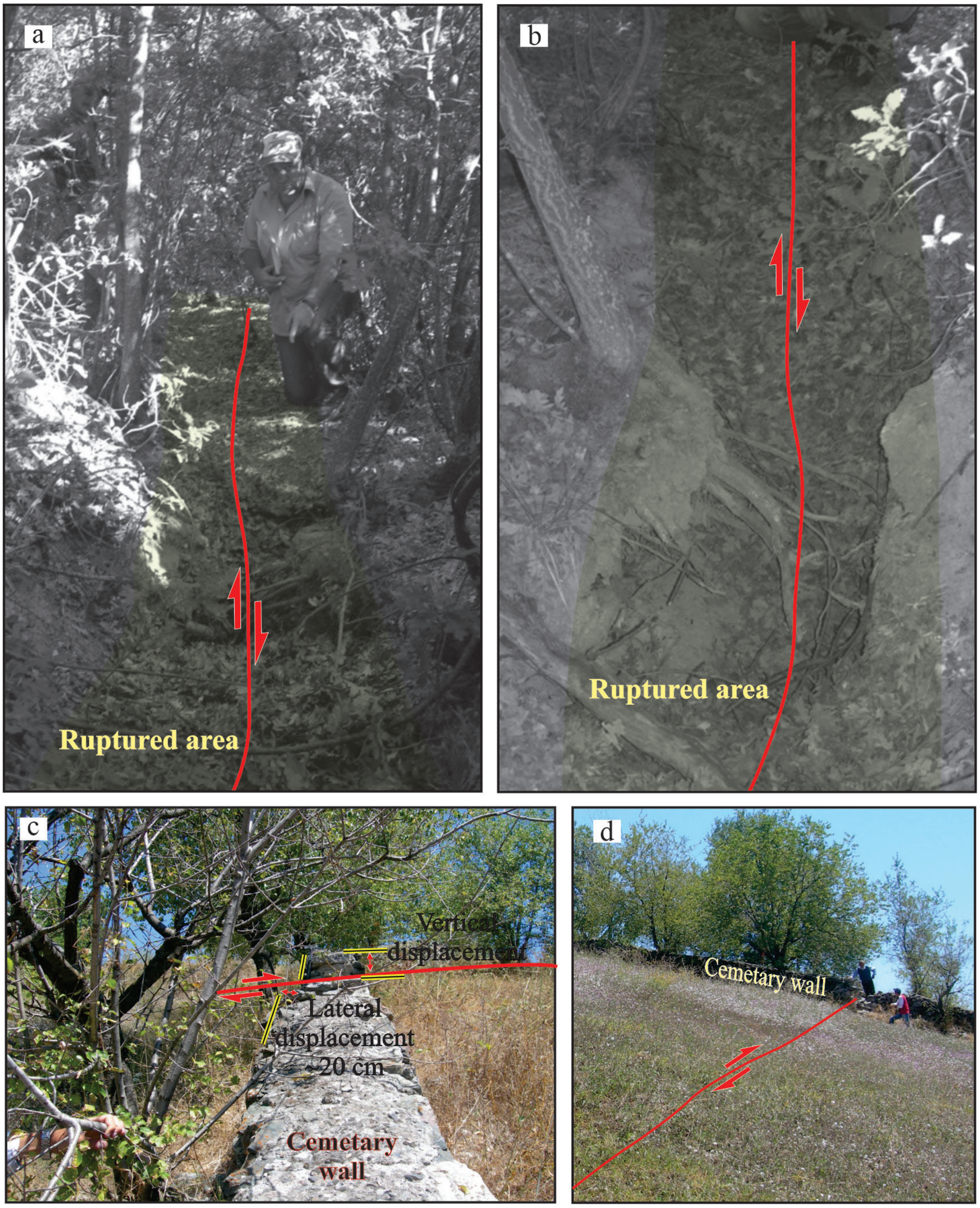

Figure 5. After 83 years, clearly observed 1939 rupture on the Ezinepazarı fault. a-b: The general view of surface rupture in Efeköy, at the Mantar Evlekliği locality. c-d: The view of the approximately 20 cm right lateral offset in the form of creep on the west wall of the Gökçeyol village cemetery.

related wedge in the trenches and six samples taken from the soil surface covering these levels (Table 1).

The T1 trench was opened according to the observations made on this natural cut (Figures 6a–6c). From this point, the fracture that continues towards the west of Yağmurlu village crosses the Kemer River and continues in the Gökçeyol village.

The fault plane was measured as N64W/62NE in the measurement made where the fault trace is very well observed in the Maşık Pınarı locality located in the south of Ambarcık Tepe between Gökçeyol and Yağmurlu villages. At this point, the T3 trench was opened (Figure 6). From the striations observed on this fault plane, it was determined that the fault had a right lateral strike-slip

Table 1. Paleoseismological trench locations and sample numbers in this study.

Trench no.	Trench location	Coordinate	Trench location altitude	Sample no.
T1	Yağmurlu village NE	44.87821 N 37.316221E	853	T1-b1, T1-b2
T2	Yağmurlu village NE	44.87851 N 37.45285E	857	T2-a2, T2-a3
T3	Between Gökçeyol and Yağmurlu	44.88597 N 37.312492 E	935	T3-4, T3-5

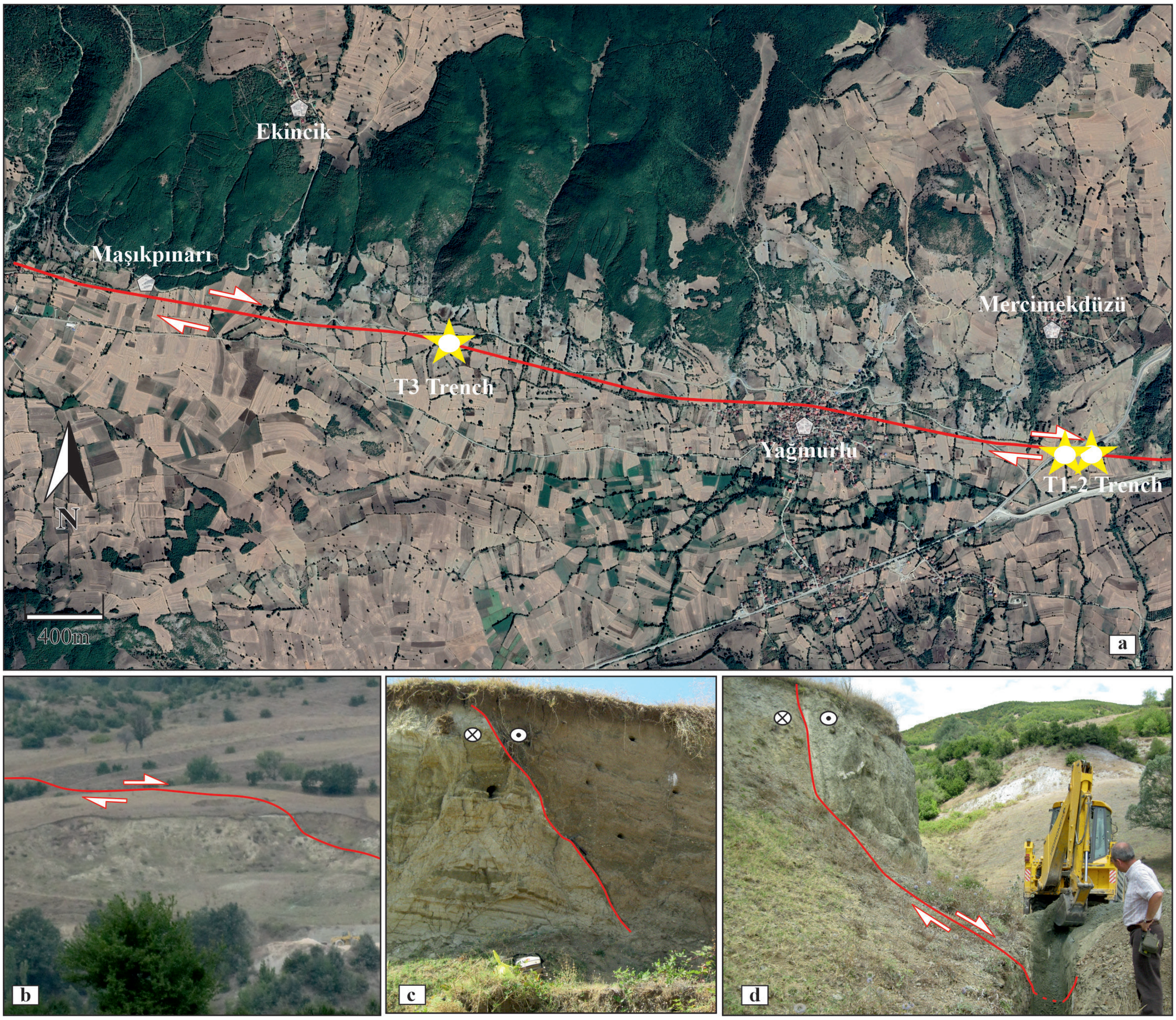

Figure 6. a) The image showing the T1, T2, and T3 trench locations. The active faults are redrawn from Emre et al. (2013). b) Close-up view of the T2 location that used natural cut. c-d) The trace of the 1939 earthquake surface rupture and close-up view of the T3 trench location. It is noted that two different units are juxtaposed on the natural cut and trench locations.

character with a small amount of vertical component. In the observations made in the Gökçeyol village, the fracture trace continues inside the village, and the vertical and lateral translations formed on the wall of the cemetery are an indication that the fracture is still moving. According to the information given by the villagers, the walls of the cemetery were built about 20 years ago, and the lateral offset on the wall was measured at about 20 cm. The fracture continues in Ortaköy and Ezeköy, which is further west than Gökçeyol village.

The surface rupture that continues along Ezeköy has made a stepover at the crossing of the Kuyucak stream and a sag pond has formed in the area. The fault trace continues from north of Efeköy and landslides are observed in the area to the north of the fracture. Continuing west from Efeköy, the fracture enters the Yenice village, approximately 200 m south of Armutarası locality. In this section, the fault trace extending along the south of Küçükdik Tepe also cuts the main road in the Köşeli district and continues westward between Şehitler Tepe and Canbolat village by jumping right. A sag pond was formed in the stepover zone. At the same time, the offset river and elongated ridge morphology can be clearly observed in the region (Figure 2). The related fault trace continues from this point towards the west, from north of the Canbolat village. Barka (1996) stated in his study that the slip of the related fault in the vicinity of Canbolat was between 1.5 and 2 m. The fracture continues westward from the Canbolat village in approximately E-W direction, just south of Hacıali village. It is also stated by the villagers that large rifts were formed in the 1939 earthquake in the southwest of the village. The fracture extends towards the Fındıcak village further west from here.

4.2.1. T1 natural trench

T1 trench consists of the natural road cut at 853 m elevation, northeast of the Yağmurlu village, where the fault trace is evident, and the trench (T2) opened on the fault trace observed at 30 m west of it. In the T1 natural trench site (Figure 4), N86W / 51NE fault trace is clearly observed. While the north of the T1 location is formed by EW trending ridges parallel to the extension of the fault trace, the south of the location is formed by E-W trending Sulucadere valley.

Trench T1-a was opened in the N30E direction, as 20 m long, 1 m wide and 1.6 m deep. The same fault trace in the T1 location, with decreased slope value, was measured in the central part of the natural trench, at N85W / 26NE (Figure 7).

The cut in the T1 natural trench, where the surface rupture of the 1939 earthquake can be observed, was used. No additional excavation work was carried out in the said cut, only the cleaning of the wall and log measurements were made. The trench wall is 4 m wide and 1.5 m deep.

Geological and structural pattern

In the detailed study on the T1 natural trench wall, a total of four different units were identified (Figure 7). Unit 1, which is the oldest unit, consists of yellowish brown Pliocene Çerkeş Formation, loosely cemented conglomerate, claystone and sandstone intercalation. Unit 2 consists of light-medium brown, angular gravel, clay, sand- and silt-sized material, and poorly sorted colluvial wedge. Unit 3, overlying these units, consists of wedge-shaped colluvial materials consisting of dark brown, muddy, sandy and angular gravels. Unit 4, which unconformably overlies other units at the top, is composed of 30 cm thick contemporary vegetable soil rich in organic material at the top of the wall. Many secondary minor faults located obliquely to the main fault plane of the 1939 earthquake surface rupture trace located within the Ezinepazarı fault segment are also located in the northern block of the T1 natural trench (Figures 6 and 7). In general, it can be said that these N35W trending secondary faults were developed by the effect of approximately N-S directing tensional forces during E-W directional movements of the main fault plane.

Evaluation of faulting events

The upper part of the main fault plane was filled with an old postearthquake wedge (Example: T1-b1; Figure 7) with a thickness of 175 cm and increased apparent thickness downwards. Below the wedge level, there is a colluvial material whose main fault plane is side by side as a result of previous event movements and coded sampling was made from this level (T1-b2). This sample was interpreted as a later earthquake event material from the fillings of the earthquake horizon represented by T1-b1 and T1-b2 samples opened by oblique secondary faulting.

In the study conducted in T1 natural trench, two events were determined according to the ^{14}C dating analyses (Table 2). The first of these events must have occurred before the deposition of the Unit 2. According to the age sample taken (T1-b1), this event indicates 18700 ± 120 BP. The event before the last event must have occurred after the deposition of Unit 2 (T1-b2) and before the deposition of Unit 3 (T1-b1).

According to the age data obtained, this event indicates a time interval between 18700 ± 120 BP and 8680 ± 40 BP (Figure 7). In the earthquake records of the historical period, the earthquakes that occurred in the Common Era in general were handled; however, the earthquakes that occurred Before the Common Era are not known. Therefore, in this trench, the earthquake findings that occurred Before the Common Era could not be correlated with historical earthquakes. However, within the scope of active tectonic movements, it is inevitable that the movements that cause medium- and large-magnitude earthquakes repeatedly in a long geological time period will also take place in this fault segment.

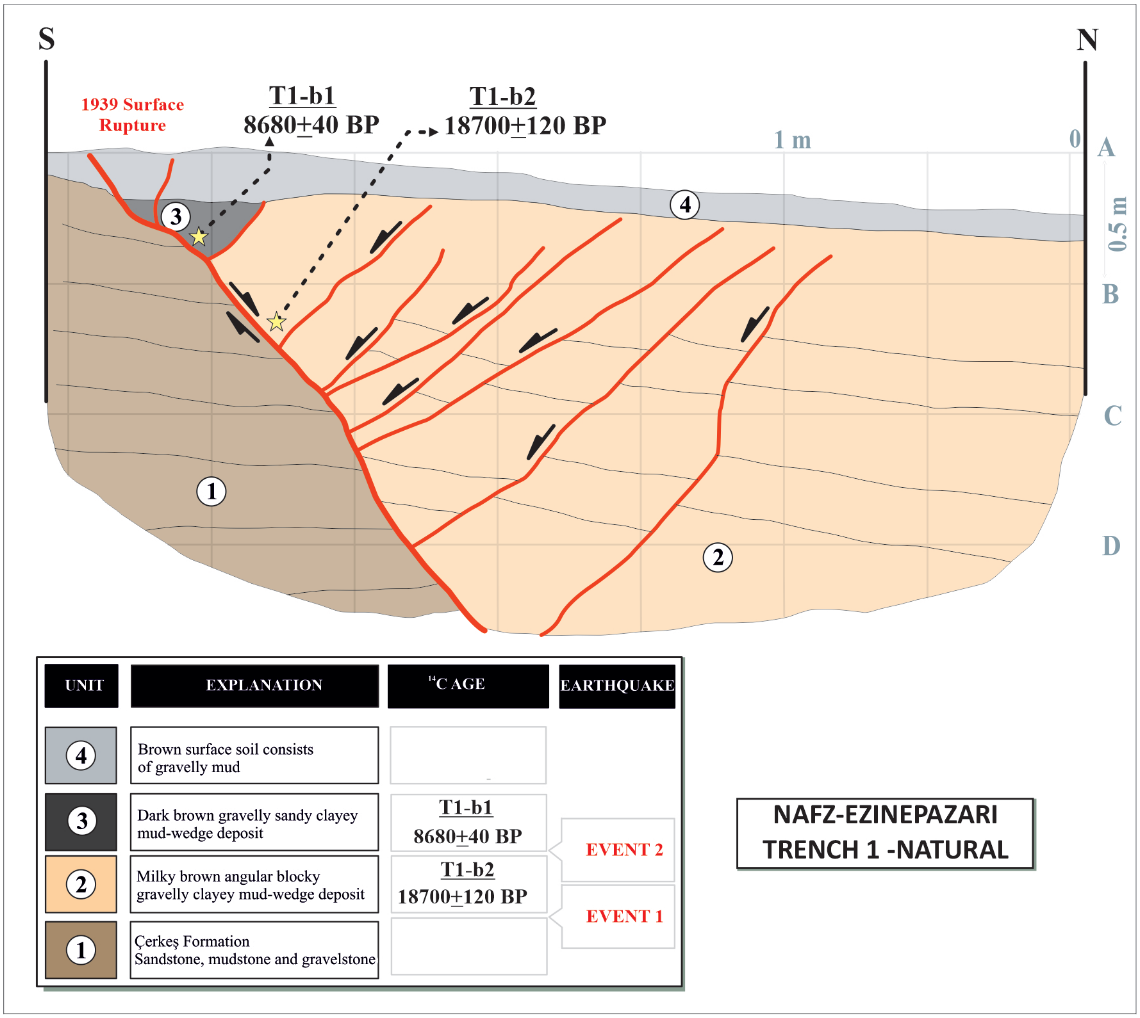

Figure 7. Trench log of west wall of trench T1 opened on the Ezinepazarı fault.

Table 2. Radiocarbon analyses and calibrated age results of samples taken from T1, T2, and T3 trenches on the Ezinepazarı fault (For calibration; OxCal 4.2 Bronk Ramsey et al. (2010); r:5 IntCal04 Atmospheric curve; Reimer et al., 2009 program was used).

Sample no.	Radiocarbon age BP	$\delta^{13}C$	Calibration	Probability 0.95 (2σ)	Type of material
T1-b1	8680 ± 40	–21.8	7788–4613 BC	95.4%	Soil
T1-b2	18700 ± 120	–25.7	21245–21224 BC	0.2%	Soil
			20959–20861 BC	1.0%	
			20701–20030 BC	93.1%	
			19995–19892 BC	1.1%	
T2-a2	15600 ± 60	–6.6	16640–16471 BC	26.4%	Soil
			16432–16076 BC	69.0%	
T2-a3	9870 ± 90	–24.8	9756–9716 BC	1.7%	Soil
			9697–9185 BC	93.7%	
T3-4	2160 ± 70	–25.1	384–47 BC	95.4%	Soil
T3-5	1660 ± 40	–19.3	AD 257–302	10.5%	Bone

4.2.2. T2 trench

T2 trench was opened in 30 m west of T1 natural trench and 4 m above with the help of an excavator. The trench is approximately 3 m long, 1.5 m wide, and 1.5 m deep.

Geological and structural pattern

A total of three units were identified in the T2 trench (Figure 8). The oldest unit forms the Pliocene Çerkeş Formation Unit 1. This unit is overlain by Quaternary sediments consisting of brown gravel, clay and sand-sized materials. The sediments forming the NE block are generally composed of angular gravels and proportionally lesser amount of sand- and silt-sized material that is less consolidated or unconsolidated. In addition, the block- or coarse-block-sized materials are rarely observed in these deposits. In the mentioned trench, Unit 1 forms the SW block of the fault and Unit 2 forms the NE block of the fault. At the top of Unit 3, a 30-cm-thick vegetation rich in organic material unconformably overlies all the units. In SW of the inclined fault plane, the lithologies of the Çerkeş Formation are generally transformed into fault breccia. Radiocarbon samples coded as T2-a2 and T2-a3 were taken from the trench wall.

Evaluation of faulting events

According to the studies, one event was detected in the trench before the 1939 earthquake. The event in question must have occurred prior to the deposition of Unit 2. The sample coded as T2-a2 was taken from inside the colluvial wedge, which is the material after the earthquake, from a depth of 125 cm from the surface and the sample of T2-a3 was taken from a depth of 110 cm from the surface. Accordingly, the event in question must have occurred between 9870 ± 90 BP and 15600 ± 60 BP (Figure 8).

4.2.3. T3 trench

T3 trench is located in NW of Maşıkpınarı between Yağmurlu and Gökçeyol villages. It was opened in the N-S direction and it is 10 m long, 1 m wide, and 1.8 m deep. In this trench, the main fault plane with N64W/62 SW was cut.

Geological and structural pattern

The work was carried out on east and west walls of the T3 trench, and only over the west wall. A total of three

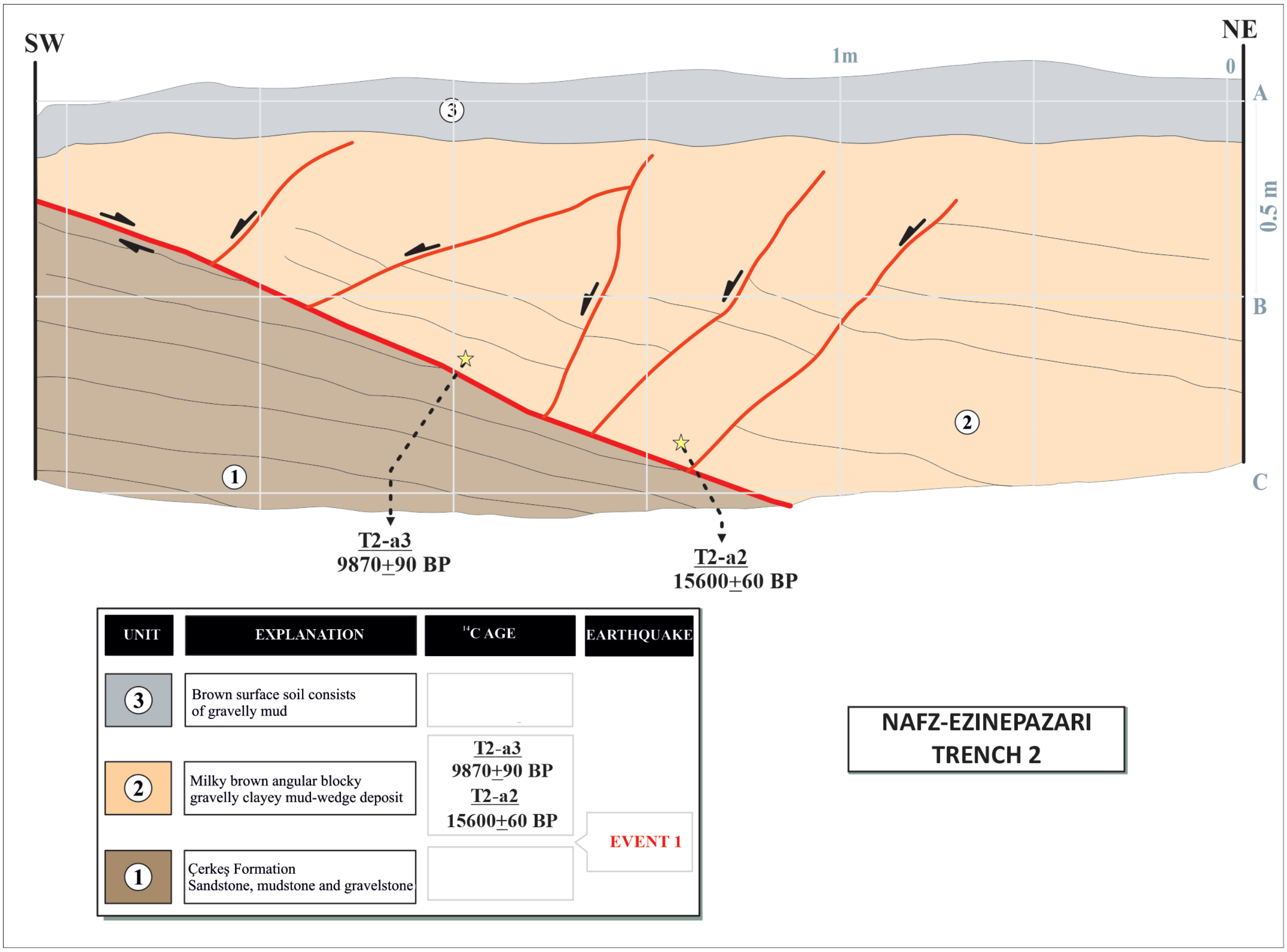

Figure 8. Trench log of the wall of T2 trench opened on the Ezinepazarı fault.

units were defined in the trench (Figure 9). Unit 1, the oldest unit, consists of Permo-Triassic Turhal Group rocks, mostly mafic magmatic rocks and recrystallized limestone blocks are characteristic on the wall. The overlying Unit 2 consists of clayey, sandy gravels of milky brown-gray color, poorly sorted gravels. Unit 3, on the other hand, consists of organic matter rich vegetable soil unconformably overlying all the units. The aforementioned fault juxtaposes Unit 1, whose northern block consists of Permo-Triassic Turhal Group rocks, and Unit 2, whose southern block consists of Quaternary terraced sediments. Samples coded as T3-4 and T3-5 were taken from the west wall of the relevant trench within Unit 2 and used in ^{14}C dating analyses.

Evaluation of faulting events

In samples taken in T3 trench study and ^{14}C dating analysis (Table 2), one event that took place before the 1939 earthquake was detected. The event in question must have occurred prior to the deposition of Unit 2. In the light of the age data determined, the event may have occurred in 2160 ± 70 BP; 1660 ± 40 BP (Figure 9). In this context, when the event in question, which took place before 464, is matched with historical earthquake catalogs, it can be

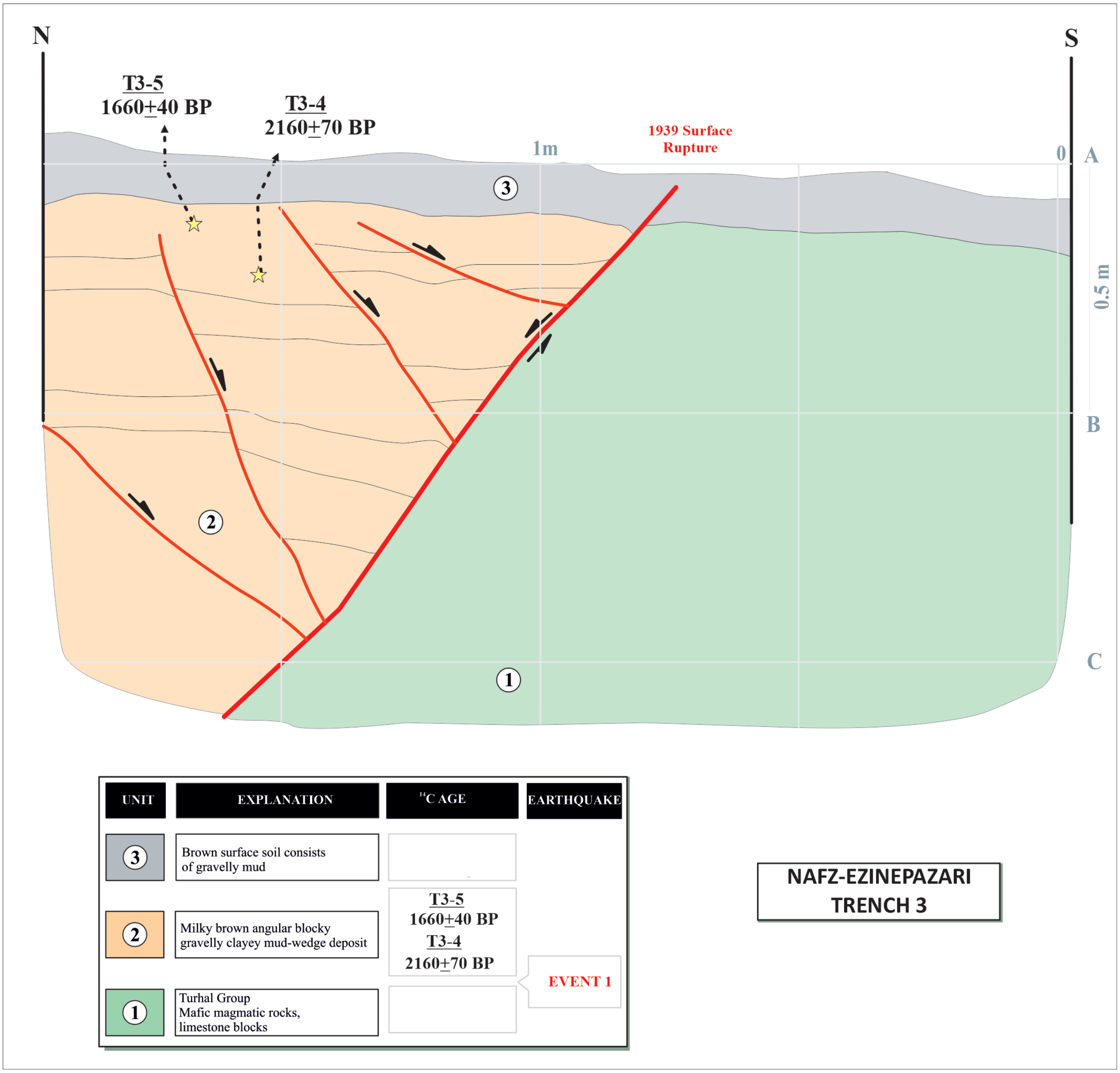

Figure 9. Trench log of the east wall of T3 trench opened on the Ezinepazarı fault.

said that it may be related to the earthquake that occurred between AD 330 and 366 and caused destruction around Niksar.

5. Discussion and conclusion

In this study, paleoseismological studies and field observations were undertaken of the 1939 Erzincan earthquake rupture segment of the NAF between Haciali village and the Derindere villages, near the preexisting investigations at Sokutas village (Emre et al., 2020) to the east. A total of three trenches were excavated on the Ezinepazari fault (EPF) in order to evaluate Holocene-Quaternary activity and delineate the earthquake recurrence interval of EPF. Based on this research, the following assessments and discussions can be made.

At least two events that occurred before the 1939 earthquake have been identified. When all detected events in the Oxcal program are evaluated together, Event 1 was found as 5871 ± 2300 BP, and Event 2 was found as 1651 ± 128 BP, yielding average interevent times of 4220 years between E1 and E2, 288 years between E2 and E3. Moreover, considering the error parameter of ages, the interevent times could be up to 6390 years. The historical earthquake obtained on the Ezinepazarı segment show that this segment has an irregular earthquake recurrence interval (Figure 10). According to the results of this study, there is one earthquake event that affected this region in the relevant time period in the historical catalogs which is the 343 Niksar earthquake. Event 1 is attributable to prehistoric earthquakes originating from the fault but not found in historical catalogs. Except for the AD 343 earthquake, the 1939 surface rupture was observed in all trenches. The surface fracture trace of the earthquake that occurred in 1668 and was felt almost everywhere in Anatolia could not be observed in trench studies. According to this result, the 1668 earthquake did not occur on the Ezinepazarı segment, and it can be concluded that the earthquake had an effect on the main segments of the North Anatolian Fault Zone further north (Table 3).

According to the historical catalogs, many of the earthquakes occurred on NAFZ (e.g., Ambraseys 1970; Ambraseys and Finkel 1987, 1995; Eyidoğan et al., 1991; Ambraseys and Melville 1994; Guidoboni et al., 1994; Guidoboni and Comastri, 2005, Tan, et al., 2008). From these earthquakes, traces of the AD 236, AD 1035-1045-1050, and AD 1668 earthquakes on the NAFZ were

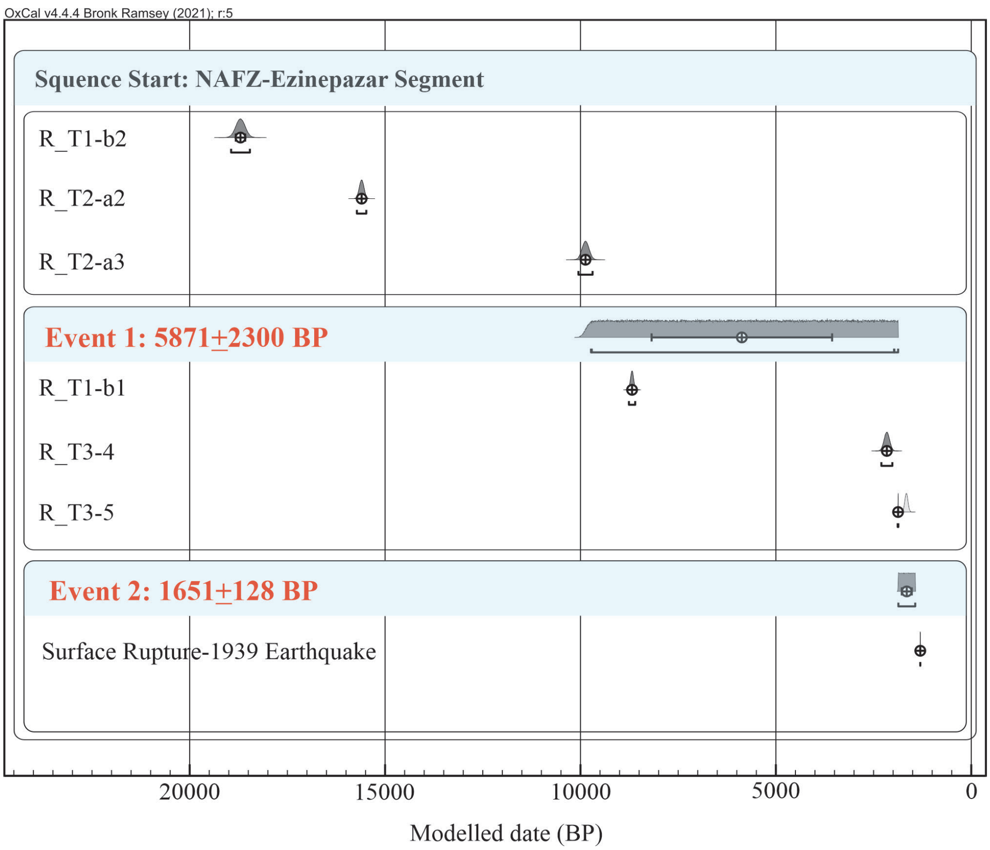

Figure 10. Statistical evaluation showing the earthquake events caused by the fault in the Oxcal program, of all data determined from the trench excavations carried out in the Ezinepazarı fault.

Table 3. The comparison of the earthquakes that occurred along all segments. These segments are grouped into NAFZ's main branch and its splays (Emre et al., 2013; 2018).

1939 earthquake surface rupture zone				
Ezinepazarı Segment (ES)	**Reşadiye Segment (RşS)**	**Suşehri Segment (SS)**	**Refahiye Segment (RfS)**	**Erzincan Segment (ES)**
AD 1939 earthquake				
AD 780–1040 earthquake (Emre et al., 2020)	AD 1668 earthquake (Fraser et al., 2009, 2012; Zabcı et al., 2011; Hubert-Ferrari et al., 2012; Kondo et al., 2012; Avşar et al., 2014)		AD 1254 earthquake (Hartleb et al., 2006; Kozacı et al., 2011)	-
AD 343 earthquake (this study)	-	-	-	-
6221–1621 BC (This Study)	-	-	-	-

detected by using trench-based paleoseismological studies (Yoshioka et al., 2000; Hartleb et al., 2003; 2006). In this study, for the first time, the trace of the AD 343 earthquake was found in the T3 trench that was conducted on the Ezinepazarı segment. This indicates that the Ezinepazarı segment may have the source of the AD 343 Niksar earthquake.

Emre et al. (2020) stated that the Sokutaş trench proposes a minimum 899 and a maximum 1159 years recurrence interval for the 1939 and penultimate earthquakes on the Ezinepazarı fault segment. Because of the fault complexity, while our result indicates an imminent recurrence interval at the minimum, Emre et al.'s study (2020) suggests a lower interval range than our results at the maximum. However, additional paleoseismological investigations are required on the Ezinepazarı segments to shed light on such a large recurrence interval.

The previous studies were divided into 1939 earthquake ruptures as five morphological segments/subsegments (Barka 1996, Emre et al., 2020). Especially Ezinepazarı fault (EPF) was grouped by Emre et al. (2020) into two different subsegments namely Canbolat and Karataş in light of McCalpin's (1996) postulated model of fault behavior segments. In this study, two stepover zones mapped along the 40 km surface rupture were investigated and the surface rupture was examined in three subsegments. All these subsegments can be evaluated within the Canbolat segments, as suggested by Emre et al. (2020). Albeit, EPF is divided into two morphological subsegments by these researchers, the postulated three subsegments well suit in light of the fault behavioral segments definition.

In the river between the mosque and the cemetery in Gökçeyol village, a displacement of approximately 25 m has been determined in this study. However, in the geological studies carried out along the North Anatolian Fault Zone (NAFZ), a total offset of 85 ± 5 km in the east of the fault zone and approximately 25 ± 5 km in the west was calculated. The displacement along the NAFZ decreases from east to west, and it is accepted that the reason for this decrease is the visible displacements of many splay faults, which generally extend into the Anatolian block from the main fault (Seymen 1975, Tatar 1978, Şengör 1979, Barka 1981, 1992, Barka and Hancock 1984, Şengör et al. 1985, Şaroğlu 1985, 1988, Koçyiğit 1988, 1990, Toprak 1989, Yaltırak 1996, Piper et al. 1997, Tüysüz et al. 1998, Armijo et al. 1999, Barka et al. 2000, Yaltırak et al. 2000). While it has been suggested that the slip rate along the NAFZ is about 5–10 mm/year (Barka 1992) or 17 ± 2 mm/year (Westaway 1994) from geological data analysis, values ranging from 30–40 mm/year have been revealed from plate movements and seismological data (Taymaz et al. 1991). On the other hand, the current GPS data show that current slip rates are between 15 and 25 mm/year (Oral et al. 1995, Ayhan et al. 1995, Reilinger et al. 1997, McClusky et al. 2000, Tatar et al. 2012). The estimates based on known GPS data give a total movement (pulses) of 75–125 km in the Recent-Pliocene interval. This value is approximately compatible with the calculated value of 85 ± 5 km (Seymen 1975, Westaway 1994, Armijo et al. 1999, Barka et al. 2000).

My study reveals that the current annual movement of the Ezinepazarı fault is associated with the observed displacement on the wall of the Gökçeyol village cemetery built 20 years ago. Accordingly, the observed 20-cm displacement shows that the relevant fault segment moves an average of 1 cm per year. This result overlaps with the findings of Tatar et al. (2012), who found as a result of their GPS study on the eastern segments of the NAFZ, with an average movement rate of 20.1 ± 2.4 mm/year and a decrease in this rate by spreading over other segments towards the west.

Moreover, according to Wells and Coppersmith's (1994) empirical equations, the EPF having the maximum potential earthquake can be delimited as 7.23, albeit Emre et al. (2018) suggested it up to 7.98 for all segments including the EPF. Considering the average recurrence interval suggests that the EPF can be categorized as class A, according to the taxonomy of Slemmons and de Polo (1986), which signifies a fault of high activity rate with excellent to well-developed geomorphic evidence of activity. Furthermore, this diagram indicates that the annual long-term slip rate can be between 1 mm/year and 10 mm/year when the estimated earthquake and recurrence interval are evaluated together.

All in all, the recent earthquake that occurred on NAFZ (23.11.2022; Mw: 5.9) has drawn attention to the recurrences interval of the NAFZ and its segments. This unexpected moderate to large earthquake signified that NAFZ's earthquake interval does not follow properly due to its complexity. For that reason, it is strongly recommended that further paleoseismological studies should be performed to well-understand the Quaternary behavior of this complex structure.

References

Ambraseys NN, Finkel C (1987). The Saros, Marmara earthquake of 9 August 1912, Journal Earthquake Engineering and Structural Dynamics 189-212.

Ambraseys NN, Finkel CF (1995). The seismicity of Turkey and adjacent areas: a historical review 1500-1800 İstanbul Muhittin Salih Eren.

Ambraseys NN, Melville CP (1995). Historical evidence of faulting in Eastern Anatolia and Northern Syria. Annali Di Geofisica XXXVIII: 337-343.

Ambraseys NN, Jackson JA (1998). Faulting associated with historical and recent earthquakes in the Eastern Mediterranean region. Geophysical Journal International 133: 390-406.

Ambraseys NN (1970). Some characteristics features of the North Anatolian Fault Zone. Tectonophysics 9: 143-165.

Armijo R, Meyer B, Barka AA, Hubert A (1999). Propagation of the North Anatolian fault into the Northern Aegean: timing and kinematics, Geology 27: 267–270.

Avşar U, Hubert-Ferrari A, Batist De M, Lepoint G, Schmidt S et al. (2014). Seismically-triggred organic-rich layers in recent sediments from Göllüköy Lake (North Anatolian fault, Turkey). Quaternary Science Reviews 103: 67-80.

Ayhan ME, Demir C, Kahveci M, Kaplan M (1995). 1990-1993 yılları GPS ölçümleri ile Gerede-Adapazarı bölgesindeki alanın belirlenmesi, in: Türk Haritacılığının 100. yılı Bilimsel Kongresi, Ankara, 55-60 (in Turkish with an abstract in English).

Barka AA (1981). Seismo–tectonic aspects of the North Anatolian Fault Zone, PhD Thesis, University of Bristol, Bristol.

Barka AA, Hancock PL (1984). Neotectonic deformation patterns in the convex-northwards arc of the North Anatolian fault zone. In: Dixon, J. G. & Robertson, A. H. F. (eds), Neotectonic deformation patterns in the convex-northwards arc of the North Anatolian fault zone. Geological Society, London, Special Publications 763-774.

Barka AA (1992). The North Anatolian Fault Zone. Annales Tectonicae 6: 164-195.

Barka AA (1996). Slip distribution along the North Anatolian Fault associated with large earthquakes of period 1939 to 1967, Bulletin of the Seismological Society of America 86/5: 1238-1254.

Barka A (2000). Paleoseismological studies along the North Anatolian Fault. Annual Meeting, Israel Geological Society 2000: 12.

Barka AA, Akyüz SH, Cohen HA, Watchorn F (2000). Tectonic evolution of the Niksar and Taşova-Erbaa pull-apart basins, North Anatolian Fault Zone: their significance for the motion of the Anatolian block, Tectonophysics 322: 243–264.

Bronk Ramsey C, Dee M, Lee S, Nakagawa T, Staff R (2010). Developments in the calibration and modelling of radiocarbon dates. Radiocarbon 52 (3): 953-961.

Emre Ö, Duman TY, Özalp S, Elmaci H, Olgun Ş et al. (2013). Active Fault Map of Turkey with an Explanatory Text [Açıklamalı Türkiye Diri Fay Haritası]. 1:1,250,000 Scale, General Directorate of Mineral Research and Exploration, Special Publication Series-30, Ankara.

Emre Ö, Duman TY, Özalp S, Şaroğlu F, Olgun Ş et al. (2018). Active fault database of Turkey. Bulletin of Earthquake Engineering 16 (8): 3229-3275. https://doi.org/10.1007/s10518-016-0041-2

Emre Ö, Kondo H, Özalp S, Elmacı H (2020). Fault geometry, segmentation and slip distribution associated with the 1939 Erzincan earthquake rupture along the North Anatolian Fault Zone. Dilek Y, Ogawa Y, Okubo Y (eds) Characterization of Modern and Historical Seismic–Tsunamic Events, and Their Global–Societal Impacts. Geological Society, London, Special Publications 501: https://doi.org/10.1144/SP501-2019-141.

Eyidoğan HU, Güçlü ZU, Değirmenci E (1991). Türkiye Büyük Depremleri Makro-sismik Rehberi (1900-1988). İstanbul Teknik Üniversitesi Maden Fakültesi Jeofizik Mühendisliği Bölümü, İstanbul 198 pp.

Guidoboni E, Comastri A, Traina G (1994). Catalogue of Ancient Earthquakes in the Medditerranean Area up to the 10th Century. INGV: Roma.

Guidoboni E, Traina G (1995). A new catalogue of earthquakes in the historical Armenian area from antiquity to the 12th century.

Guidoboni E, Comastri A (2005). Catalogues of Earthquakes and Tsunamis in the Mediterranean Area from the 11th to 15th Century. Istituto Nazionale di Geofisicae Vulcanologia Rome.

Erturaç MK, Tüysüz O (2012). Kinematics and Basin Formation along the Ezinepazar-Sungurlu Fault Zone, NE Anatolia, Turkey. Turkish Journal of Earth Sciences 21: 497-520. https://doi.org/10.3906/yer-0910-27

Hitchcock C, Altunel E, Barka AA, Bachhuber J, Lettis W et al. (2003). Timing of late Holocene earthquakes on the eastern Duzce Fault and implications for slip transfer between the southern and northern strands of the North Anatolian fault system, Bolu, Turkey. Turkish Journal of Earth Sciences 12: 119-136.

Fraser J, Pigati JS, Hubert-Ferrari A, Vanneste K, Avsar U et al. (2009). A 3000-year record of ground-rupturing earthquakes along the central North Anatolian Fault near Lake Ladik, Turkey. Bulletin of the Seismological Society of America 99 (5): 2681-2703.

Fraser J.G, Huber-Ferrari A, Verbeeck K, Garcia-Moreno D, Avsar U et al. (2012). A 3000-year record of surface-rupturing earthquakes at Günalan: variable fault-rupture lengths along the 1939 Erzincan earthquake rupture segment of the North Anatolian Fault, Turkey. Annals of Geophysics 55 (5): 895-927, doi: 10.4401/ag-4884.

Gürsoy H, Tatar O, Akpınar Z, Polat A, Mesci L, Tunçer D (2013). New observations on the 1939 Erzincan Earthquake surface rupture on the Kelkit Valley Segment of the North Anatolian Fault Zone, Turkey. Journal of Geodynamics 65: 259-271.

Hartleb R, Dolan JF, Akyüz HS, Dawson TE, Tucker AZ et al. (2002). Surface rupture and slip distributions along the Karadere segment of the 17 August 1999 İzmit and the western section of the 12 November Düzce, Turkey, earthquakes. Bulletin of the Seismological Society of America 92: 67-78.

Hartleb RD, Dolan JF, Akyüz HS, Yerli B (2003). A 2000-year-long paleoseismologic record of earthquakes along the central North Anatolian Fault, from trenches at Alayurt, Turkey. Bulletin of the Seismological Society of America 93: 1935-1954.

Hartleb RD, Dolan JF, Kozacı Ö, Akyüz HS, Seitz GG (2006). A 2500-yr-long paleoseismologic record of large, infrequent earthquakes on the North Anatolian fault at Çukurçimen, Turkey, Geological Society of America Bulletin 118: 7/8: 823-840.

Hubert-Ferrari A, Avsar U, El Ouahabi M, Lepoint G, Martinez P et al. (2012). Paleoseismic record obtained by coring a sag-pond along the North Anatolian Fault (Turkey). Annals of Geophysics 55 (5): 929-953. https://doi.org/10.4401/ag-5460.

Ketin İ (1969). Kuzey Anadolu Fayı Hakkında. Maden Tetkik ve Arama Dergisi 72: 1-27.

Klinger Y, Sieh K, Altunel E, Akoglu A, Barka AA et al. (2003). Paleoseismic evidence of characteristic slip on the western segment of the North Anatolian Fault, Turkey. Bulletin of the Seismological Society of America 93: 2317-2332.

Koçyiğit A, Tokay M (1985). Çatalçam (Zevker)-Erzincan arasında Kuzey Anadolu fay Kuşağı'nın sismo-tektonik incelenmesi. Fay kuşağının stratigrafisi, sistematiği ve neotektonik özellikleri: Bayındırlık ve İskan Bakanlığı, Araştırma ve Uygulama Genel Müdürlüğü, Proje Kod No: 82-04-08-00-02: 101s (In Turkish).

Koçyiğit A (1988). Basic geologic characteristics and total offset of the North Anatolian Fault Zone in Suşehri area, NE Turkey, METU Pure and Applied Sciences 22: 43–68.

Koçyiğit A (1989). Suşehri basin: an active fault-wedge basin on the North Anatolian Fault Zone, Turkey, Tectonophysics 167: 13–29.

Koçyiğit A (1990). Tectonic setting of the Gölova basin, total offset of the North Anatolian Fault Zone, Eastern Pontides, Turkey, Annales Tecton. 4: 155-170.

Kondo H, Özalp S, Elmacı H, Emre Ö (2012). The high-resolution paleoseismic record on the 1939 surface rupture, North Anatolian Fault system, Turkey. AOGS – AGU (WPGM) Joint Assembly, 13-17 August 2012, Abstract Book, SE57-A007, Resorts World Sentosa, Singapore.

Kondorskaya NV, Ulomov VI (1999). Special Catalogue of Earthquakes of the NorthernEurasia (SECNE). http://www.seismo.ethz.ch/gshap/neurasia/nordasiacattxt, Access date: 25.01.2009.

Kozacı Ö, Dolan JF, Yönlü Ö, Hartleb RD (2011). Paleoseismologic evidence for the relatively regular recurrence of infrequent, large-magnitude earthquakes on the eastern North Anatolian fault at Yaylabeli, Turkey. Lithosphere 3: 37-54.

Mccalpin JP (1996). Application of paleoseismic data to seismic hazard assessment and neotectonic research. In: Palaeoseismology (Ed: JP. McCalpin), Academic Press, 439-493, ISBN: 0-12-481826-9.

McClusky S, Balassanian S, Barka AA, Demir C, Georgiev I et al. (2000). GPS contraints on crustal move- ments and deformations in the eastern mediterranean (1988–1997): implications for plate dynamics. Journal of Geophysical Research 105: 5695–5719.

Oral MB, Reilinger RE, Toksoz MN, King RW, Barka AA et al. (1995). Global positioning system offers evidence of plate motions in Eastern Mediterranean. EOS 7 (2): 9–11.

Palyvos N, Pantosti D, Zabcı C, D'Addezio G (2007). Paleoseismological Evidence of Recent Earthquakes on the 1967 Mudurnu Valley Earthquake Segment of the North Anatolian Fault Zone. Bulletin of the Seismological Society of America 97: 1646-1661.

Pantosti D, Pucci S, Palyvos N, Martini PMD, D'Addezio G et al. (2008). Paleoearthquakes of the Düzce fault (North Anatolian Fault Zone): Insights for large surface faulting earthquake recurrence. Journal of Geophysical Research 113: B01309-B01309.

Parejas E, Akyol İH, Altınlı E (1942). Le tremblement de terre d'Erzincan du 17 Decembre 1939, Rev. Fac. Sci. Univ. lstanbul NVI: 177-222 (in French).

Pavlides SB, Chatzipetros A, Tutkun ZS, Ozaksoy V, Dogan B (2006). Evidence for late Holocene activity along the seismogenic fault of the 1999 Izmit earthquake, NW Turkey. Geological Society Special Publications 260: 635-647.

Piper JDA, Tatar O, Gürsoy H (1997). Deformational behaviour of Continental Lithosphere deduced from block rotations across the North Anatolian Fault Zone, Turkey. Earth and Planetary Science Letters 150: 191-203.

Reilinger R, McClusky S, Oral B, King R, Toksöz MN et al. (1997). Global positioning system measurements of present-day crustal movements in the Arabia–Africa–Eurasia plate collision zone. Journal of Geophysical Research102: 9983–9999.

Reimer PJ, Baillie MGL, Bard E, Bayliss A, Beck JW et al. (2009). IntCal09 and Marine09 radiocarbon age calibration curves, 0-50,000 years cal BP. Radiocarbon 51(4): 1111-1150.

Pamir HN, Ketin İ (1941). Das Anatolische Erdbeden Ende 1939. Geolog Rundsch 32: 278-287 (in German).

Polat A, Tatar O, Gürsoy H, Karabacak V, Zabçi, C et al. (2012). 1939 Erzincan depremi yüzey kırığının Ortaköy-Suşehri segmenti üzerinde paleosismolojik bulgular. Kuzey Anadolu fay zonu. Türkiye Jeoloji Bülteni 55 (3): 137-157 (in Turkish).

Slemmons DB, de Polo CM (1986). Active tectonics. Washington (DC): National Academy Press.

Seymen İ (1975). Kelkit vadisi kesiminde Kuzey Anadolu Fay Zonu'nun tektonik özelliği. Ph.D. Thesis ITÜ 192 pp (in Turkish).

Şaroğlu F (1985). Geological and Structural Evolution of East Anatolia during Neotectonic Period, PhD Thesis, İstanbul Univesity, İstanbul, (unpublished; in Turkish with an abstract in English).

Şaroğlu F (1988). The age and offset on the North Anatolian Fault. METU Pure and Applied Sciences 21: 65-79.

Şengör AMC (1979). The North Anatolian Transform Fault: its age, offset and tectonic significance. Journal of the Geological Society 136: 269-282.

Şengör AMC, Görür N, Şaroğlu F (1985). Strike-slip faulting and related basin formation in zones of tectonic escape: Turkey as a case study. In: Biddle, K.T. and Christie-Blick, N. (eds) Strike-slip Faulting and Basin Formation. Special Publication: Society of Economic Paleontologists and Mineralogists 37: 227–264.

Tan O, Tapirdamaz MC, Yoruk A (2008). The earthquake catalogues for Turkey. Turkish Journal of Earth Sciences 17: 405-418.

Tatar Y (1978). Tectonic study of Erzincan-Refahiye section of the North Anatolian Fault Zone. Hacettepe University Earth Sciences 4: 201-236 (in Turkish with an abstract in English).

Tatar O, Poyraz F, Gürsoy H, Çakır Z, Ergintav S et al. (2012). Crustal deformation and kinematics of the Eastern Part of the North Anatolian Fault Zone (Turkey) from GPS measurements Tectonophysics 518–521: 55-62.

Taymaz T, Jacson J, McKenzie DP (1991). Active tectonics of the North and Central Aegean Sea. Geophysical Journal International 106: 433-490.

Tüysüz O, Barka AA, Yiğitbaş E (1998). Geology of the Saros Graben its implications on the evolution of the North Anatolian Fault in the Ganos-Saros region, NW Turkey. Tectonophysics 293: 105-126.

Wells DL, Coppersmith KJ (1994). New empirical relationships among magnitude, rupture length, rupture width, rupture area, and surface displacement. Bulletin of the seismological Society of America 84 (4): 974-1002.

Westaway R (1994). Present-day kinematics of the Middle East and Eastern Mediterranean. Journal of Geophysical Research 99: 12071-12090.

Yaltırak C (1996). Tectonic history of the Ganos Fault System. Turkish Association of Petroleum Geologists Bulletin 8: 137-156 (in Turkish with an abstract in English).

Yaltırak C, Sakınç M, Oktay FY (2000). Kinematics and evolution of the northern segment of the North Anatolian Fault Zone (Ganos Fault) in the area between Marmara and Gulf of Saroz. in Tatar O, Kavak KŞ, Özden S (Eds.), Tektonik Araştırma Grubu 3. Toplantısı, ATAG-3 Proceedings, pp. 77-89 (in Turkish with an abstract in English).

Yaşar HH (1912-1928). Amasya tarihi, 4 cilt, Necm-i İstikbal Matbaası, İstanbul 846 (in Turkish).

Yoshioka T, Okumura K, Kuşçu İ, Emre Ö (2000). Recent surface faulting of the North Anatolian Fault along the 1943 Ladik earthquake ruptures. Bulletin of the Geological Survey of Japan 51: 29-35.

Zabcı C, Akyüz HS, Karabacak V, Sançar T, Altunel E et al. (2011). Palaeoearthquakes on the Kelkit Valley segment of the North Anatolian Fault, Turkey: Implications for the surface rupture of the historical 17 August 1668 Anatolian Earthquake. Turkish Journal of Earth Sciences 20: 411-427.